

Surprisingly Large Generation and Retention of Helium and Hydrogen in Pure Nickel Irradiated at High Temperatures and High Neutron Exposures - L. R. Greenwood, F. A. Garner, and B. M. Oliver (Pacific Northwest National Laboratory), M. L. Grossbeck (Oak Ridge National Laboratory), and W. G. Wolfer (Lawrence Livermore National Laboratory)

OBJECTIVE

The objective is to predict and measure gas production in fusion relevant materials.

SUMMARY

Hydrogen and helium measurements in pure nickel irradiated to 100 dpa in HFIR at temperatures between 300 and 600°C show higher gas concentrations than predicted from fast-neutron reactions and the two-step $^{58}\text{Ni}(n,\gamma)^{59}\text{Ni}$ (n,p and n, α) reactions. This additional gas production suggests previously unidentified nuclear sources of helium and possibly hydrogen that assert themselves at very high neutron exposure. The elevated hydrogen measurements are especially surprising since it is generally accepted that hydrogen is very mobile in nickel at elevated temperatures and therefore is easily lost, never reaching large concentrations. However, it appears that relatively large hydrogen concentrations can be reached and retained for many years after irradiation at reactor-relevant temperatures. These new effects may have a significant impact on the performance of nickel-bearing alloys at high neutron fluences in both fission and fusion reactor irradiations.

PROGRESS AND STATUS

Introduction

Until recently, the production and retention of helium and hydrogen in nickel, iron, and stainless steels was thought to be well predicted by the combination of fast neutron (n,He) and (n,H) reactions as well as the well-known two-step $^{58}\text{Ni}(n,\gamma)^{59}\text{Ni}$ (n,p and n, α) reactions. The ^{59}Ni reaction is a prolific source of helium that has been used to achieve helium to dpa (displacements per atom) ratios that simulate fusion reactor conditions in mixed-spectrum fission reactor irradiations. Earlier helium measurements in the High Flux Isotopes Reactor (HFIR) appeared to be in good agreement with calculations and neutron dosimetry measurements up to thermal neutron fluences of about 4×10^{22} n/cm². [1-2] Recently, however, new helium measurements at much higher thermal neutron fluences up to 1.1×10^{23} n/cm² show an excess of helium over the predictions. Furthermore, measurements using a new hydrogen system developed recently at PNNL [3], have shown that pure nickel samples irradiated to the same high fluences also have more hydrogen than would be predicted. These elevated hydrogen measurements are especially surprising since hydrogen is thought to be very mobile at the temperatures of the HFIR experiments so that the hydrogen would diffuse out of the samples, never reaching the levels observed in our measurements.

Impact on Materials Research

The two-step nickel reaction can produce high levels of helium and hydrogen in stainless steels and Inconel in fission reactor components irradiated to high neutron fluences. These reactions are also widely used to produce helium in stainless steels in mixed spectrum fission reactor irradiations in order to simulate the helium to dpa ratios expected for a fusion reactor. In both cases, confident prediction of the gas production, as well as the increased dpa due to the energetic recoils, is clearly required for the understanding of material property effects that may arise from the trapped helium. It is well known that helium and other gases stabilize small vacancy clusters to form bubbles and void cavities, thereby accelerating the onset of void swelling. Recently, it has been proposed that hydrogen can also perform

* Pacific Northwest National Laboratory (PNNL) is operated for the U.S. Department of Energy by Battelle Memorial Institute under contract DE-AC06-76RLO-1830.

this role. [4] Furthermore, it has been suggested that hydrogen may influence the development of irradiation assisted stress corrosion cracking, although no convincing evidence of hydrogen's direct role has yet been provided. The high levels of hydrogen seen in these measurements strongly suggest that hydrogen may be trapped in the voids and cavities along with the helium. [4]

Neutron Irradiations and Reactor Dosimetry

All of the samples used for the hydrogen and helium measurements were high purity nickel wires used for neutron dosimetry in various HFIR materials irradiation experiments for US and Japanese fusion reactor materials programs. [5] Typically, reactor dosimetry capsules containing small milligram-sized wires of Fe, Ni, Ti, Nb, and Co-Al alloy were placed at various elevations in materials irradiation assemblies located in either the peripheral target position or removable beryllium positions of HFIR. These wires were analyzed to determine activation rates that were used to adjust the neutron fluence spectra at each location of the reactor dosimetry capsules. Consequently, the neutron exposures are very well known for all of the samples used to measure helium and hydrogen that are cited in this paper. It is important to note that both the thermal and fast neutron fluences must be well-known since the total gas production in nickel is due to both the $^{58}\text{Ni}(n,\gamma)^{59}\text{Ni}(n,p)$ and n,α two-step thermal reactions as well as the more conventional fast neutron $(n,\text{hydrogen})$ and (n,helium) reactions, which include all fast neutron reactions that lead to gas production. Since the reactor dosimetry measurements are non-destructive, the nickel dosimeters could be used subsequently to measure both the helium and the hydrogen contents.

Helium Measurements

The helium was measured with high accuracy by isotope dilution mass spectrometry at PNNL. Samples were slightly acid etched to remove surface effects, then melted in a furnace to release all of the helium gas. A known ^3He spike was added and the ratio of ^3He to ^4He was used to determine the absolute number of ^4He atoms in the samples. Some of the helium data at lower neutron fluences [1] was originally measured at Rockwell International prior to the move of the helium analysis system from Rockwell to PNNL in 1996. All of the helium measurements for pure nickel samples irradiated in HFIR are shown as a function of the thermal neutron fluence in Figure 1. The measured helium values range up to about 35,000 appm or about 3.5 at%. The stainless steel dpa values are shown near each helium measurement since stainless steel dpa is typically used as an exposure parameter for the HFIR irradiations. The dpa values for the pure nickel samples would be considerably higher, up to about 100 dpa, due mainly to the extra dpa from the high energy recoil from the $^{59}\text{Ni}(n,\alpha)$ reaction. The Ni dpa values are 59, 78, and 104 for the corresponding stainless steel values of 34, 44, and 59 dpa shown on

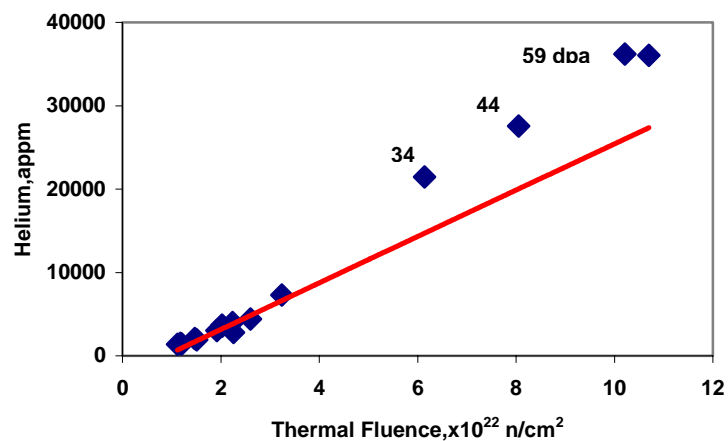


Figure 1. Measured and calculated helium production from nickel irradiated in HFIR. The solid line is calculated using the evaluated ^{59}Ni cross sections.

Figure 1. The line in Figure 1 represents the standard calculation of helium from nickel, as will be discussed in more detail below.

Hydrogen Measurements: A new hydrogen analysis system was developed at PNNL in 1999. [3] This system heats samples to approximately 1200°C to release the hydrogen without melting or vaporizing the samples. Hydrogen leak standards are used to calibrate the system. In addition to rapid hydrogen release at a fixed temperature, hydrogen can also be measured as a function of increasing temperature. Figure 2 shows that most of the hydrogen in pure irradiated nickel is released by 700°C, well below the maximum temperature used to extract the hydrogen from the irradiated nickel samples. The hydrogen measurements for pure nickel irradiated in HFIR are shown in Figure 3. The diamonds show the measured values while the circles show the calculations using the standard model, as described below. The dpa values shown on the figure again refer to stainless steel rather than nickel since the HFIR experiments involved mainly stainless steel samples. As can be seen, the measured hydrogen values exceed the predicted values in all cases over the range of temperatures from 300 to 600°C. It should be noted that the excess hydrogen seen in the samples could be due to environmental sources rather than simply nuclear production. The HFIR samples are not in contact with water, which is known to produce copious amounts of hydrogen through radiolysis in water reactors. However, at the elevated temperatures of the HFIR experiments, hydrogen is very mobile so that the samples have a flux of hydrogen moving through them during the experiment. The main point is that some of this hydrogen must be retained at the end of the experiment, contrary to our usual expectations. It should also be mentioned that the exact temperature values are not known since the dosimetry capsules were located between experimental capsules that had temperature monitoring. The dosimeters are believed to have temperatures between the values of the adjacent experimental assemblies, although exact values are not available.

Calculated Helium and Hydrogen Production in Nickel: The production of helium and hydrogen in nickel, iron, and stainless steel has been discussed previously. [1,2] The fast and thermal neutron (n,H) and (n,He) cross sections for natural nickel were obtained from the ENDF/B-VI data files, which include ^{59}Ni as well as the natural isotopes.[6] The cross sections for individual nickel isotopes, are shown in Figures 4, 5, and 6. It is noteworthy that the gas production cross sections for natural nickel are not appropriate for these high fluence irradiations in HFIR since there is significant transmutation both between the various nickel isotopes as well as the production of many non-nickel isotopes. Figure 7 shows a schematic representation of the isotopes that are produced by high fluence thermal neutron irradiations of pure nickel, including both stable and radioactive products. Gas production calculations at high neutron fluences must then take into effect the transmutation between the various Ni isotopes as well as transmutation to isotopes of other elements.

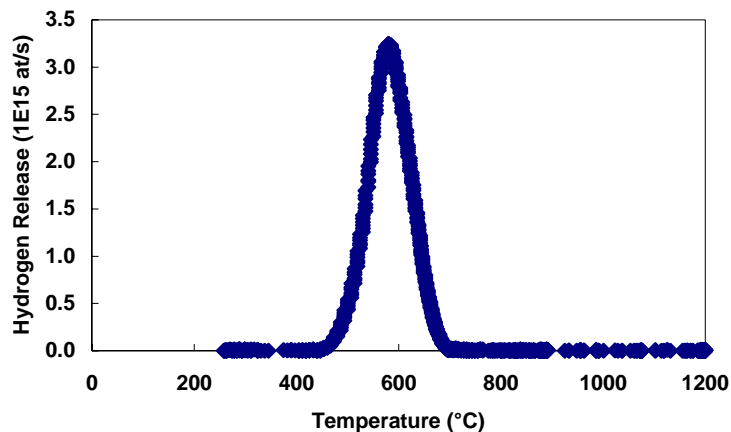


Figure 2. Hydrogen release from irradiated nickel sample as a function of temperature.

Most of the transmutation, as shown in Figure 7, that occurs in these high fluence irradiations consists of neutron capture (n,γ) reactions that have the effect of increasing the isotopic abundances of the higher-mass nickel isotopes as well as the radioactive isotopes ^{59}Ni and ^{63}Ni . As can be seen from Figures 5 and 6, the burnout of ^{58}Ni to ^{59}Ni increases the net fast neutron gas production, as well as the

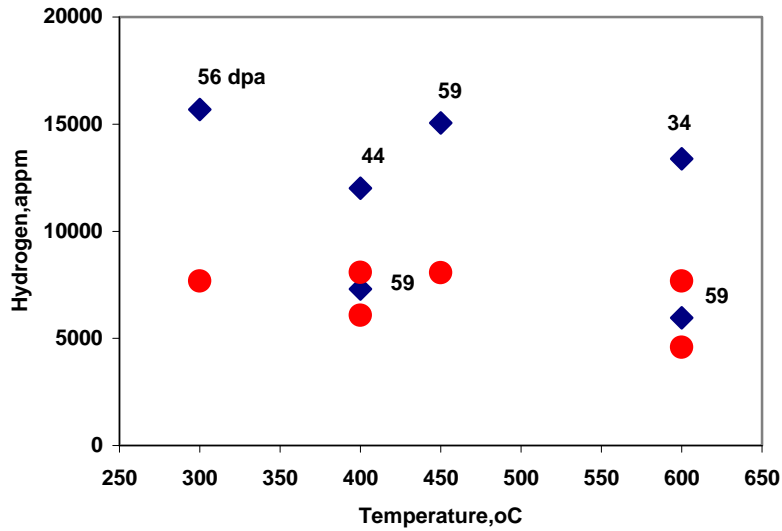


Figure 3. Measured (diamonds) and calculated (dots) hydrogen in nickel irradiated in HFIR to various 316SS dpa values.

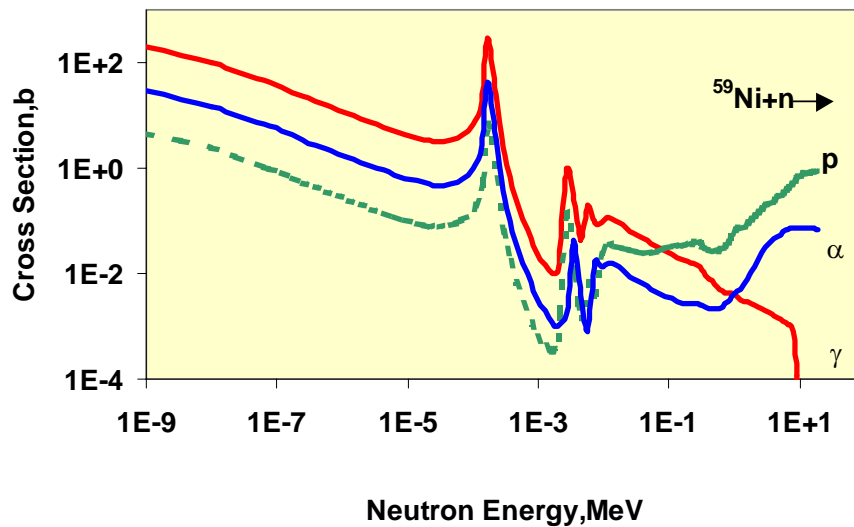


Figure 4. Evaluated neutron cross sections for ^{59}Ni from ENDF/B-VI.

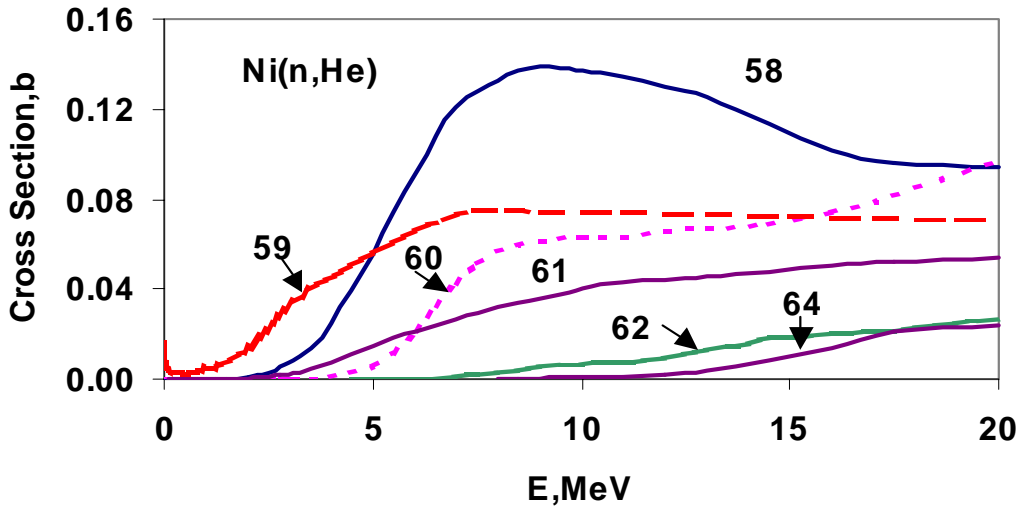


Figure 5. Total helium production cross sections for the nickel isotopes.

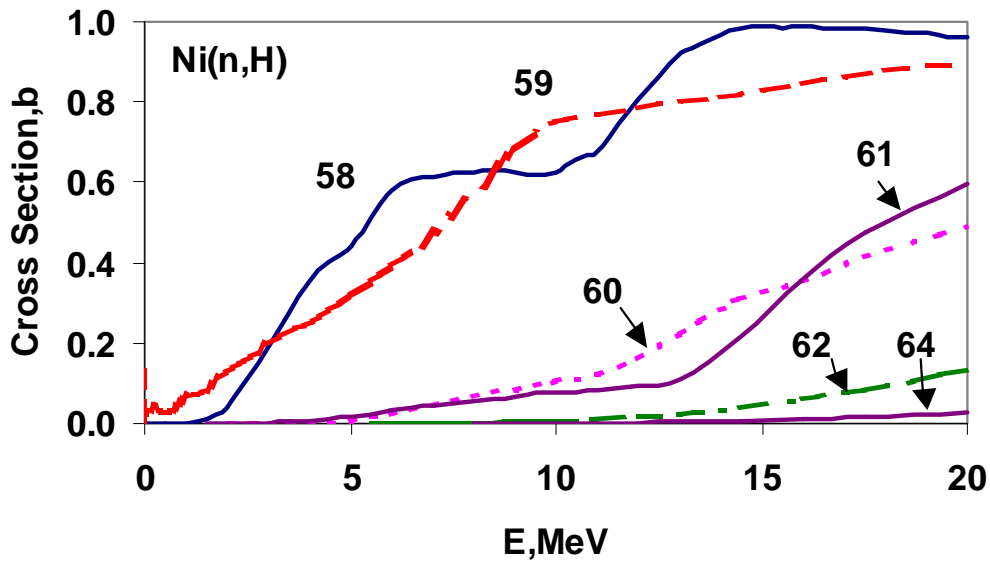


Figure 6. Total hydrogen production cross sections for the nickel isotopes.

thermal neutron production. However, at increasingly higher neutron fluences, as both the ^{58}Ni and ^{59}Ni are consumed, the net fast neutron gas production from Ni will actually decrease since the higher mass nickel isotopes have lower cross sections. The gas production from ^{63}Ni has not been measured or calculated. However, based on the Q-values, these reaction cross sections are thought to be similar to those for the other, higher mass nickel isotopes. All of the hydrogen and helium calculations were performed by integrating the various cross sections in figures 4-6 over the HFIR neutron energy spectra, then combining the fast neutron and ^{59}Ni reactions to get the total gas production.

The uncertainties in the ^{59}Ni cross sections listed in Table 1 cannot explain the differences seen between the measured and calculated helium data, especially in light of new ^{59}Ni measurements presented below. Uncertainties in the neutron fluences determined by the reactor dosimetry measurements are also too small to explain the excess helium production; especially since all of the HFIR data have the same systematic sources of uncertainty.

Mass Spectrometry Measurements of ^{59}Ni

In order to rigorously test the ^{59}Ni total absorption cross section, the nickel isotopic ratios were measured by thermal ionization mass spectrometry for the nickel samples irradiated to high exposures in HFIR and the results are listed in Table 2. The samples were dissolved in acid and the nickel fraction was separated by ion exchange reactions. The separated nickel fractions were then loaded onto filaments and heated to measure the nickel isotopic ratios. An unexpected interference from copper was seen at mass 63 and 65. Consequently, ^{63}Ni was measured separately by liquid scintillation counting to properly normalize the data. The net uncertainty on the ^{59}Ni content of the samples is estimated to be only 1%.

The ^{59}Ni content only depends on the production cross section from ^{58}Ni and the total absorption or burnup cross section and decay of ^{59}Ni . As shown in Table 1, the $^{58}\text{Ni}(n,\gamma)^{59}\text{Ni}$ cross section is quite well known. Consequently, the ^{59}Ni data in Table 2 rigorously tests the ^{59}Ni total absorption cross section. Table 2 also lists the calculated ^{59}Ni content in the samples using the evaluated cross sections, as explained above. As can be seen, the ^{59}Ni measurements and the calculations are in excellent agreement with $\text{C/M} = 1.017 \pm 0.009$, much better agreement than might be expected from the uncertainties in the cross sections listed in Table 2. The measured data and calculations are also in excellent agreement (within $\pm 2\%$) for ^{58}Ni and ^{60}Ni , as shown in Figure 8. The fit to the data can be improved slightly by raising the ^{59}Ni total absorption cross section by 1.6% to 93.5 barns. However, this adjustment is within the estimated 2% 2- σ uncertainty in the TIMS data and is not justified considering the other uncertainties in the calculation due to both the ^{58}Ni cross section as well as the neutron fluence measurements. Furthermore, increasing the ^{59}Ni absorption cross section lowers the helium production from nickel, increasing the discrepancy with the helium measurements. The conclusion is that the ^{59}Ni nickel cross sections predict concentrations that are in excellent agreement with the ^{59}Ni measurements. Consequently, uncertainties in the nickel cross sections cannot explain the discrepancy between the helium measurements and calculations.

Other Possible Sources of Helium: Since we have demonstrated that the ^{59}Ni cross sections correctly predict the isotopic concentrations, the most probable explanation for the excess helium production at high neutron fluences is that a daughter or granddaughter isotope produced by transmutation from natural nickel may produce helium. Figure 7 shows a section of the table of isotopes surrounding nickel. The blank isotopes are stable, those shown in gray and pink are radioactive, and those shown in pink are the best candidates for an unknown source of helium or hydrogen. In order to compete with the ^{59}Ni reactions, a candidate isotope would need to have a significant thermal neutron (n,α or n,p) reaction.

Table 2. Measured and Calculated ^{59}Ni Content of Irradiated Ni in HFIR

Nickel Sample	Thermal Fluence, $\times 10^{22}$ n/cm ²	Measured ^{58}Ni Atom% ^a	Measured ^{60}Ni Atom% ^a	Measured ^{59}Ni Atom% ^a	Calculated ^{59}Ni Atom%	^{59}Ni Ratio C/M
Natural	0	68.1	26.2	0		
JP15-42	6.14	53.2	34.2	2.59	2.66	1.03
JP12-24	8.05	48.8	37.1	2.46	2.48	1.01
JP15-41	10.21	44.9	39.0	2.26	2.28	1.01
JP12-39	10.70	43.8	39.6	2.19	2.24	1.02

^aMeasurements by thermal ionization mass spectrometry are accurate to $\pm 1\%$.

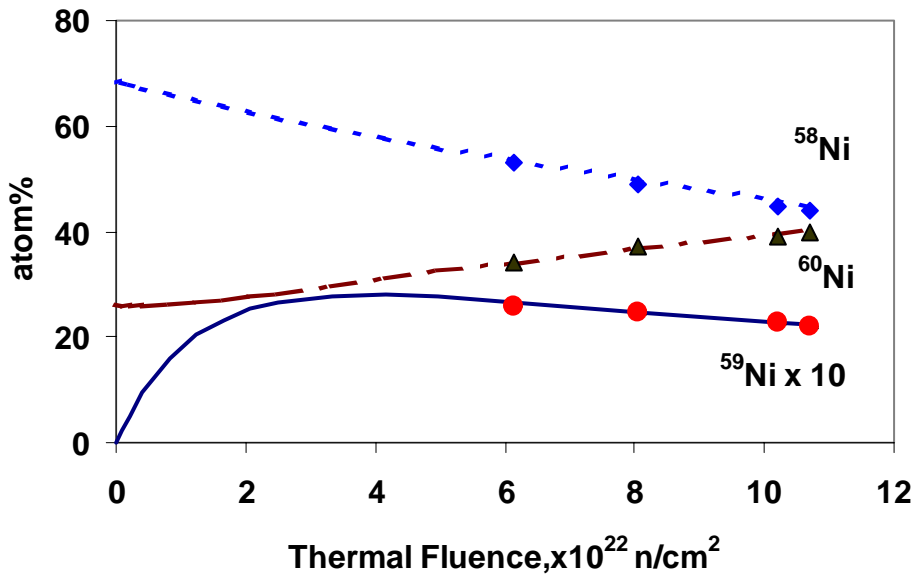


Figure 8. Comparison of measured and calculated nickel isotopic concentrations as a function of the thermal neutron fluence. Note that the ^{59}Ni values are multiplied times 10.

All known isotopes that have thermal neutron (n, α) or (n,p) cross sections lie on the proton-rich side of the line of stability on the Chart of the Nuclides. Furthermore, a candidate isotope must have a large positive Q-value for the reaction of interest, as shown in Table 3. These criteria lead to the selection of ^{55}Fe , ^{57}Co , ^{58}Co , and ^{65}Zn as the only possible candidates. All of the other radioactive isotopes in Figure 7 (besides ^{59}Ni) are either too short-lived or have unfavorable Q-values. ^{65}Zn is known to have a thermal neutron cross section for helium and most likely for hydrogen, as well. [7] However, the production of ^{65}Zn from nickel is much too small to explain the excess gas seen in our experiments. Similarly, ^{55}Fe is thought to have a small thermal (n, α) cross section of about 0.011 barns [8]; however, again the production of ^{55}Fe is not enough to explain the excess gas production. This leaves only ^{57}Co and ^{58}Co as reasonable candidates. The (n, α) Q-value is too low for ^{57}Co , although this isotope could be a source of additional hydrogen. ^{58}Co is known to have a very high (n, γ) cross section of 1900 barns and the Q-values are high enough that it could produce H and He, as well. However, the (n, α) and (n, p) thermal neutron cross sections would have to be very large in order to compete with the rapid elimination of ^{58}Co due to decay (78 day) and transmutation to ^{59}Co .

Table 3. Thermal Neutron Q-Values and Cross Sections

Isotope	(n, α) Helium Reactions		(n,p) Hydrogen Reactions	
	Q,MeV	Thermal σ ,b	Q,MeV	Thermal σ ,b
Ni-59	5.096	12.0	1.855	1.96
Zn-65	6.481	4.7	2.134	?
Fe-55	3.584	0.011	1.014	?
Co-58	3.511	?	3.089	?
Co-57	1.858	?	1.618	?

FUTURE WORK

Additional measurements are needed to determine the production of hydrogen and helium from nickel at high neutron fluences. The data in Figure 1 could be used to make an empirical correction to high fluence predictions, but only in the fluence range shown. In order to confidently predict helium production at much higher neutron fluences, a more detailed understanding of the reaction mechanisms will be required. If a daughter or granddaughter isotope produces the excess gas, then the effect may be very non-linear, as is the case for ^{59}Ni . Gas measurements are needed at higher neutron fluences, especially for separated nickel isotopes as well as daughter or granddaughter isotopes in order to explain the excess gas production that we have measured.

ACKNOWLEDGEMENTS

This work was supported by the U.S. Department of Energy, Office of Fusion Energy, under Contract DE-AC06-76RLO 1830. Pacific Northwest National Laboratory is operated for DOE by Battelle Memorial Institute. This work was also performed under the auspices of U.S. DOE by the University of California, Lawrence Livermore National Laboratory under contract N. W-7405-Eng-48.

REFERENCES

- [1] L. R. Greenwood, *Journal of Nuclear Materials*, 115, pp. 137-142, 1983.
- [2] L. R. Greenwood, D. W. Kneff, R. P. Skoronski, and F. M. Mann, *Journal of Nuclear Materials*, 123, pp. 1002-1010, 1984.
- [3] B. M. Oliver, F. A. Garner, L. R. Greenwood, and J. A. Abrefah, High-Sensitivity Mass Spectrometer System for the Determination of Hydrogen in Irradiated Materials, *Journal of Nuclear Materials* 283-287, pp. 1006-1010, 2000.
- [4] F. A. Garner, B. M. Oliver, L. R. Greenwood, D. J. Edwards, and S. M. Bruemmer, 10th International Conference on Environmental Degradation of Materials in Nuclear Power Systems, 2002; submitted for publication in *Journal of Nuclear Materials*.
- [5] L. R. Greenwood and C. A. Baldwin, *Fusion Materials Semiannual Progress Report for Period Ending December 31, 1997*, DOE/ER-0313/23, pp. 301-304, 1998.
- [6] Evaluated Nuclear Data File, Version VI, National Nuclear Data Center, Brookhaven National Laboratory.
- [7] D. W. Kneff, L. R. Greenwood, D. W. Skowronski, and F. M. Mann, *Radiation Effects*, Vols. 92-96, pp. 553-556, 1986.
- [8] L. R. Greenwood, D. G. Graczyk, and D. W. Kneff, *Journal of Nuclear Materials* 155-157, p. 1335, 1988.